

600817
60000

FTD-TT-

64-258

TT - 64-11672

12-P-#0.50

TRANSLATION

A METHOD OF LIQUID JET BLOWOUT UNDER HIGH PRESSURE

By

A. A. Semerchan and N. A. Plotnikov

FOREIGN TECHNOLOGY DIVISION



AIR FORCE SYSTEMS COMMAND

WRIGHT-PATTERSON AIR FORCE BASE

OHIO

UNEDITED ROUGH DRAFT TRANSLATION

A METHOD OF LIQUID JET BLOWOUT UNDER HIGH PRESSURE

BY: A. A. Semerchan and M. A. Plotnikov

English Pages: 11

SOURCE: Inzhenerno-Fizicheskiy Zhurnal, (Russian), Vol. 6,
Nr. 8, 1963, pp. 82-87

5/0170-063-006-008

THIS TRANSLATION IS A RENDITION OF THE ORIGINAL FOREIGN TEXT WITHOUT ANY ANALYTICAL OR EDITORIAL COMMENT. STATEMENTS OR THEORIES ADVOCATED OR IMPLIED ARE THOSE OF THE SOURCE AND DO NOT NECESSARILY REFLECT THE POSITION OR OPINION OF THE FOREIGN TECHNOLOGY DIVISION.

PREPARED BY:

TRANSLATION DIVISION
FOREIGN TECHNOLOGY DIVISION
WP-AFB, OHIO.

BLANK PAGE

A METHOD OF LIQUID JET BLOWOUT UNDER HIGH PRESSURE

A. A. Semerchan and M. A. Plotnikov

↓
A hydropneumatic apparatus which has a liquid jet blowout at a velocity of 2000 m/sec and higher is described below. ~~We submit~~ experimental data on measuring the velocity of turbine oil up to 1850 m/sec. ()

is submitted ↗

It is of great scientific and practical interest to obtain a free liquid jet of high velocity (1000 m/sec and higher). Works are available on a pulse jet blowout of water into air at a velocity up to 400 m/sec [1-5].

Research at the High-Pressure Physics Institute, AN SSSR, in the field of hydraulic compressors [6] which can supply working pressures in a high-pressure cylinder up to one GN/m² and higher and of appropriate sealing systems have enabled us to develop an apparatus (Fig. 1) which has a free liquid jet blowout at a velocity of 2000 m/sec and higher.

The apparatus consists of a pressure multiplier made up of two coaxial cylinders whose pistons are rigidly interconnected; consequently, at piston equilibrium in any intermediate position, the pressures in the cylinders are inversely proportional to the areas

of these pistons. The low-pressure cylinder diameter is $D_1 = 50$ mm; the high-pressure cylinder diameter is $D_2 = 10$ mm; the multiplication coefficient is $f = 25$; the piston stroke of the high-pressure cylinder is $s = 20$ mm; the useful volume of the high-pressure chamber is 1.57 cm^3 ; the low pressure cylinder is calculated for a pressure of 80 MN/m^2 with multiple safety factors. The high-pressure cylinder is a one-layered, thick-walled vessel made from 45KhNMFA steel and is subjected to pressure up to 2000 MN/m^2 , while the stresses caused by this in its walls, computed by the usual methods for a thick-walled tube, exceeds the tensile strength. Both cylinder bodies are rigidly joined together by four bolts which are designed for tensile stress corresponding to a pressure of 2000 MN/m^2 . The high-pressure cylinder piston is made from the same steel and hardened to a hardness of $R_c = 40-45$. The piston side surfaces are ground. The seal of the high pressure chamber consists of a set of alternating copper and lead rings which are subjected to hydrostatic compression by a special structure consisting of a yoke and sealing nut (Fig. 1).

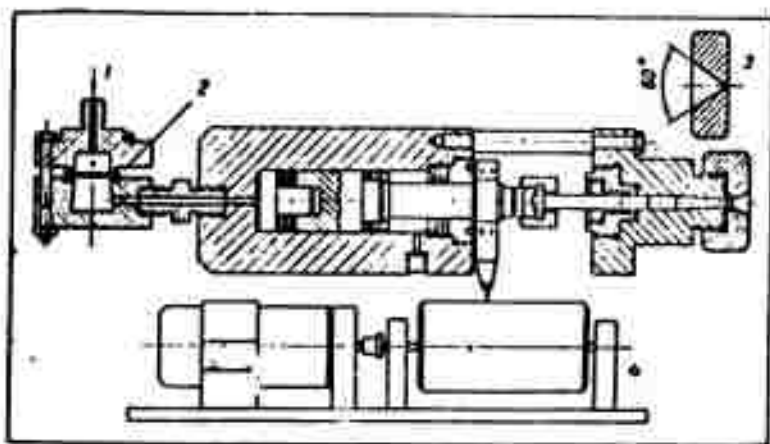


Fig. 1. A general view of an apparatus for blowout of a free liquid jet with supersonic velocity:
 1) compressed air; 2) diaphragm; 3) outlet nozzle;
 4) automatic recording instrument.

The exit nozzle with a microaperture of 0.1 mm diameter was made from 30KhGSA steel and hardened to $R_c = 50$. The configuration of the nozzle's internal surface is shown in Fig. 1. The size and configuration of the nozzle aperture was carefully measured under an instrument microscope within an accuracy to 0.001 mm. The chamber of the low-pressure cylinder, charged with compressed air at 80 MN/m^2 , is equipped with a capping seal which works on the uncompensated-area principle. This seal consists of a cap placed in the piston aperture and a set of alternating chlorovinyl and textolite rings. The chamber is sealed by compressing the rings by the pressure force on the butt end of the cap from the direction of the working gas or liquid in that chamber. The seal works well when a viscous oil is used as the working liquid. To ensure constant pressure when liquid is flowing from the nozzle, we had to charge the low-pressure cylinder with compressed air, which had been pumped first into an auxiliary tank. Here the capping seal didn't work, since air, having sufficiently low viscosity, penetrates the spaces between the cap and the rings and balanced by its own pressure the force of pressure on the head surface of the cap. Therefore, the capping seal rings were glued together, and then the whole set was glued to the surface of the cap and the piston. This ensured a completely hermetic chamber to be charged with compressed air. The return stroke chamber of the low-pressure cylinder, charged with air at $5\text{--}6 \text{ MN/m}^2$, has two sealing structures consisting of a set of alternating textolite and chlorovinyl rings, compressed by special nuts.

Figure 2 schematically depicts the system of supplying air, precompressed to a given pressure, to the apparatus. The system

consists of a hydraulic pump delivering 4 liters/hr at 80 MN/m^2 , a reservoir of working fluid (oil), two tubular helical coils, connecting tubes and shutoff valves. Coils A and B are charged with compressed air at $10\text{-}12 \text{ MN/m}^2$ by fan 5, which separates the system from the main line of compressed air. For this purpose, valves 1, 3, and 6 are closed, and valve 2 is opened. After charging the system, close valves 2 and 5 and start the pump, which forces oil from reservoir C into coil A and also compresses the air there to 80 MN/m^2 in a closed volume. Then open valve 2 and part of the air in coil A will flow into coil B. After the pressures in coils A and B equalize, close valve 2 and open 5 and 6. Then the oil contained in coil A will flow into reservoir C under the pressure of compressed air. After draining the oil from A, close valves 5 and 6 and then again start the hydraulic pump. Repeat this whole operation in the same sequence several times until the air pressure in coil B attains the proper level. Then trip triggering mechanism D and the air from coil B rushes at great speed into the chamber of the low-pressure cylinder. The size of coils A and B is selected so that to attain a pressure of $70\text{-}75 \text{ MN/m}^2$ in coil B 5-6 separate pumpings are needed. A gas-dynamic calculation of the process of air flow from coil B into the low-pressure cylinder chamber indicates that up to a piston velocity of 3 m/sec we can discount the effect of intransient flow from coils 12 meters long. The piston velocity in our experiments was $0.06\text{-}0.25 \text{ m/sec}$. The air pressure in coils A and B and in the low-pressure cylinder was measured by a manometer within 0.5 accuracy. The high pressure thus obtained was determined by the multiplication coefficient with consideration of the friction

forces on all seals.

The construction of the triggering mechanism is shown in Fig. 1. The basic element of the mechanism is a molded diaphragm placed in a special holder and held between two tapered surfaces by bolts. This fastening of the diaphragm ensures an air-tight joint and also creates conditions for hydrostatic stress in the diaphragm material. This guarantees that for a given pressure drop the diaphragm will burst instantaneously, and that after the rupture the aperture will have the correct circular form and even edges. It is easy to regulate the pressure level at which it will burst by different thicknesses of the diaphragm.

The diaphragms were made from steel and used in an unhardened state, since hardening produced minute fragments which could fall into the chamber of the working cylinder and scratch its internal surfaces. The flat part of the diaphragm has a diameter of 30 mm; for this a 1-2 mm range of thickness corresponds to a 20-80 MN/m² range of bursting pressure (in the low-pressure chamber).

We also carried out tests using a different type of triggering mechanism based on putting bursting diaphragms at the exit to the high-pressure chamber. In this case the diaphragms were placed between the nozzle contact surfaces and the covering nut. Using these sheet-iron diaphragms heat-treated in various manners caused the burst apertures to be of different sizes and configurations every time, which gave added resistance to the ejected fluid. A test using shaped diaphragms with ringed undercutting gave good results relative to the size and configuration of burst aperture. However, in this case the diaphragm burst pressure barely depended on the diaphragm thickness, but to a considerably larger degree

depended on the heterogeneity in the microstructure of the materials.

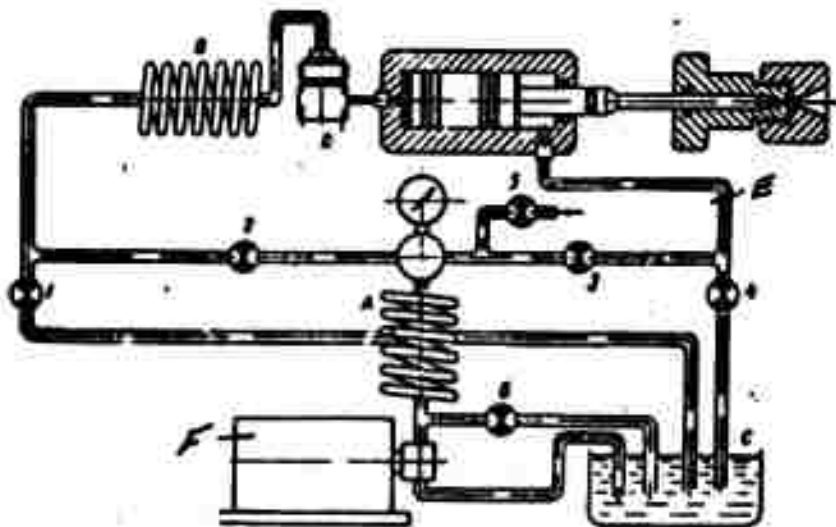


Fig. 2. The system for supplying the apparatus with air under low pressure.
E) the main compressed air line; F) a HZhR pump.

We also carried out tests with copper bushings of various lengths with steel plugs of different configurations molded into them to lock the high-pressure chamber.

This mechanism also gave negative results. With cylindrical plugs the mechanism triggered at about 500 MN/m^2 regardless of the bushing length or the pressurizing force. Also, when the plug has a molded side surface, a large part of the bushing material (copper) is forced out behind the plug through the aperture in the covering nut. As a result the nozzle slides into the cavity that is made and the hermetic seal of the high-pressure chamber is broken. An automatic recording instrument in the form of a rotating drum

(Fig. 1) parallel to the axis of the apparatus is used to determine the discharge rate from the nozzle. During operation the pattern of piston motion is recorded on the constantly turning drum by a needle rigidly fixed to the piston. The drum surface is covered with a thin layer of plasticine. To measure the drum rotational speed, a hole is drilled perpendicular to the axis in the free end of the roller. A lamp casts light on a photocell through this hole. When the drum rotates, the light is interrupted with a frequency proportional to the rotational speed. Electric current from the photocell is supplied to a frequency meter having a 1.5 accuracy class. The high-pressure chamber is filled with oil by syringe through a 3-mm diameter hole.

The work process of the apparatus after the diaphragm bursts consists of two periods. At first the piston moves irregularly, compressing the oil in the high-pressure chamber to a given density (Fig. 3, a). This period averages about 0.01 sec. During this time 5% of the fluid held in the chamber leaks from the nozzle. Then, after a very brief vibrating process, the period of uniform piston motion begins, accompanied by fluid flow under constant pressure. The length of this period depends on chamber pressure and the area of the exit aperture; in the test this period lasted 0.05-0.14 sec.

The dependence of the turbine-oil flow velocity on the pre-flow pressure is given in Fig. 3, b. Evidently the true curve of dependence of oil flow velocity on pre-flow pressure is located between the curves. An exact calculation of the true curve is impossible since there is no equation of state for turbine oil under high pressures. The dependence of density on pressure, used

to calculate curve 2, was determined by Levitt's isotherm equation for high pressures. This equation was derived empirically for various substances from Bridgeman's experimental data and has this form: $P = C \exp B \gamma_0$

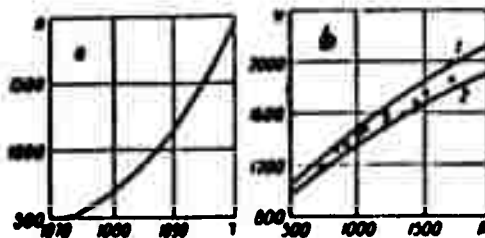


Fig. 3. The dependence of turbine oil density (kg/m^3) on pressure P (MN/m^2) at $t = 15^\circ \text{C}$, calculated according to Levitt's isotherm equation (a), and the theoretical (solid lines) and experimental (dots) dependence of turbine oil flow velocity V (m/sec) on pre-flow pressure P (MN/m^2) (b):
 1) According to Bernoulli's equation without consideration of compressibility ($\gamma_0 = 903 \text{ kg/m}^3 = \text{const}$ and is equal to the density under normal conditions);
 2) the flow calculated by the hypothesis that $\gamma_0 = \text{const}$ in the flow process, where γ_0 is the pre-flow oil density.

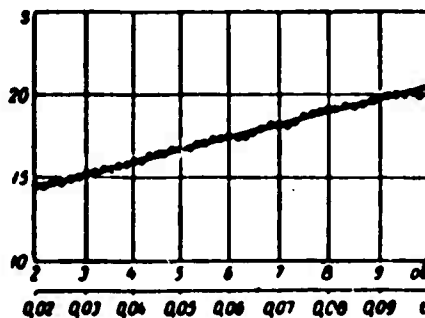


Fig. 4. A graph of the piston motion law during turbine oil flow under high pressure (s in mm, t in sec).

It has been shown [7] that this equation agrees very well with the experimental data not only for a great number of gases and liquids, but also for solids under pressures from 300 MN/m² to 10 GN/m². The values for coefficients B and C for turbine oil were determined experimentally on the apparatus with a closed outlet from the high-pressure chamber, by recording on a drum the piston movements under various pressures with consideration of the elastic deformations of the piston.

The true flow velocity of the oil from the nozzle in the steady-state process is defined by the equation of flow rate constancy for the flow outlet section and the cross section coincident with the surface of the piston head. The piston velocity is determined by the appropriate marks on the drum and by measuring the velocity of its return (Fig. 4). The oil density in the high pressure chamber is determined from the graph in Fig. 3, a; the exit aperture area is determined on an instrument microscope within an accuracy to 0.001 mm. The oil density in the outlet section was assumed equal to its density at atmospheric pressure, which holds true only for subsonic flow conditions. If in reality the oil flow velocity under high pressures somewhat exceeds the critical velocity, then the true density of the outflow oil is somewhat higher than it is at atmospheric pressure; however this difference cannot be significant. Evidently, here the values obtained for flow velocity must be considered somewhat understated. The internal surface configuration of the nozzle having a ratio of the microcanal length to its diameter approximately equal to unity was selected in order to decrease the hydraulic drag as much as possible and to ensure sufficient wall strength. As is evident from Fig. 3, b, for this

configuration of the nozzle's internal surfaces, the hydraulic resistance did not have a noticeable effect on oil flow velocity.

REFERENCES.

1. B. Dunne and B. Cassen. J. of Appl. Phys., 25, No. 5, 1954.
2. B. Dunne and B. Cassen. J. of Appl. Phys., 27, No. 6, 1956.
3. A. A. Semerchan, L. F. Vereshchagin, et al. IFZh, No. 3, 1960.
4. A. A. Semerchan. IFZh, No. 2, 1960.
5. A. A. Semerchan, L. F. Vereshchagin, et al. ZhTF, 28, No. 9, 1958.
6. L. F. Vereshchagin and V. Ye. Ivanov. PTE, No. 1, 1960.
7. L. S. Levitt. J. Phys. Chem., 58, No. 7, 1954.